Mon. Not. R. Astron. Soc. **000**, 000–000 (0000) Printed 18 September 2013 (MN LATEX style file v2.2)

Rapidly Fading Supernovae from Massive Star Explosions

Io K. W. Kleiser[1⋆], and Daniel Kasen[2,3]†,
[1]*Department of Astronomy, California Institute of Technology, Pasadena, CA 91125.*
[2]*Lawrence Berkeley National Laboratory, 1 Cyclotron Road, Berkeley, CA 94720.*
[3]*Department of Physics, University of California, Berkeley, CA 94720.*

arXiv:1309.4088v1 [astro-ph.HE] 16 Sep 2013

18 September 2013

ABSTRACT

Transient surveys have recently discovered a class of supernovae (SNe) with extremely rapidly declining light curves. These events are also often relatively faint, especially compared to Type Ia SNe. The common explanation for these events involves a weak explosion, producing a radioactive outflow with small ejected mass and kinetic energy ($M \sim 0.1$ M$_\odot$ and $E \sim 0.1$ B, respectively), perhaps from the detonation of a helium shell on a white dwarf. We argue, in contrast, that these events may be Type Ib/c SNe with typical masses and energies ($M \sim 3$ M$_\odot$, $E \sim 1$ B), but which ejected very little radioactive material. In our picture, the light curve is powered by the diffusion of thermal energy deposited by the explosion shock wave, and the rapid evolution is due to recombination, which reduces the opacity and results in an "oxygen-plateau" light curve. Using a radiative transfer code and simple 1D ejecta profiles, we generate synthetic spectra and light curves and demonstrate that this model can reasonably fit the observations of one event, SN 2010X. Similar models may explain the features of other rapidly evolving SNe such as SN 2002bj and SN 2005ek. SNe such as these require stripped-envelope progenitors with rather large radii ($R \sim 20\ R_\odot$), which may originate from a mass loss episode occurring just prior to explosion.

1 INTRODUCTION

As more powerful wide field optical surveys come online, not only have the rates of supernova (SN) discoveries increased, but so has our ability to detect rarer events at greater distances and with lower luminosities. Of particular interest is a small but growing collection of unusual supernovae whose light curves are relatively dim and of short duration. These rapidly fading supernovae (RFSNe) not only have peculiar light curves, but their spectra are also often distinctive, in some cases containing line features that have not yet been securely identified. Presumably these transients have something interesting to tell us about the life and death of stars, but we still do not have a complete understanding of their physical properties or origins.

The class of RFSNe is diverse and may be broken up into several subclasses. In this paper, we focus on SN 2010X (Kasliwal et al. 2010) and similar events, which have been found in spiral galaxies and so could potentially be related to massive star death. The peak absolute magnitude of SN 2010X was -17 (corresponding to a luminosity of $\sim 10^{42}$ erg s^{-1}) and the light curve declined very rapidly after peak (by 0.23 ± 0.01 mag day^{-1}). The spectra showed line features of oxygen, calcium, and iron, with some uncertain features attributed to perhaps aluminum or helium. The light curve of a seemingly related event, SN 2002bj (Poznanski et al. 2010), was about two magnitudes brighter than SN 2010X but declined at a nearly equal rate. The spectra of SN 2002bj contained features of silicon, sulfur, and what was tentatively identified as vanadium. In both cases, the typical ejecta velocities, measured from the blueshift of the absorption lines, were around $5,000 - 10,000$ km s^{-1}. Recently Drout et al. (2013) presented detailed observations of SN 2005ek, which strongly resembles SN 2010X in many ways.

Other RFSNe likely belong to distinct sub-classes. Events like SN 2005E have been labeled "calcium-rich transients" (Perets et al. 2010; Kawabata et al. 2010; Kasliwal et al. 2012), as their late time spectra are dominated by calcium emission. These SNe have been found in the outskirts of elliptical galaxies with no signs of star formation and therefore likely originate from old stellar populations. Another class of RFSNe, the "SN 2002-cx-like", or "Iax" events, show some spectroscopically similarities to SNe Ia, but are distinguished by low peak magnitudes (between about -14 and -19 in V-band) and low ejecta velocities (Foley et al. 2013).

Several physical models have been proposed to explain the RFSNe. In almost all cases, the rapid evolution of the light curves is explained as a consequence of a low ejected mass (~ 0.1 M$_\odot$), resulting in a short photon diffusion time through the ejecta. The ".Ia" model, for example, considers the detonation of a thin shell of helium that has accreted onto the surface of a carbon/oxygen (C/O) white dwarf (Bildsten et al. 2007; Shen et al. 2010). The model is so named because the kinetic energy (~ 0.1 B, where 1 B $= 10^{51}$ erg) as well as the ejected mass and luminosity

© 0000 RAS

are each about a tenth of those of a typical Type Ia supernova (SN Ia). This model can reproduce some basic properties of the SN 2010X light curves (Kasliwal et al. 2010). However, as we discuss later, the model has difficulty reproducing important features of the observed spectra and the shape of the light curve. In addition, current ".Ia" models do not reach the higher luminosities seen in events like SN 2002bj.

Partial explosions of C/O white dwarfs near the Chandrasekhar mass have also been suggested as an origin of RFSNe. Kromer et al. (2013) simulate a centrally ignited deflagration which burns a portion of the star but does not release enough nuclear energy to completely unbind it. Instead, a fraction of the mass (~ 0.4 M$_\odot$) is ejected with low kinetic energy and a ^{56}Ni content of ~ 0.1 M$_\odot$. The resulting transients are dim but have fairly long diffusion times due to the relatively high amount of ejected matter and low energy. The light curves therefore do not decline rapidly enough to match the SN 2010X-like events, although this model may explain the SN 2002cx-like transients.

Another potentially relevant model is the accretion-induced collapse (AIC) of a white dwarf to a neutron star. In the AIC simulations of Dessart et al. (2006), only a very small amount of radioactive material ($\sim 10^{-4} - 10^{-3}$ M$_\odot$) is ejected. The resulting transient should therefore be very dim. The simulations of (Fryer et al. 2009), however, find larger radioactive masses (~ 0.05 M$_\odot$) and predict brighter SNe. For rapidly differentially rotating white dwarfs, a centrifugally supported disk may form during collapse and subsequently be blown apart, perhaps synthesizing even more ^{56}Ni (Metzger et al. 2009; Darbha et al. 2010; Abdikamalov et al. 2010). In these models, the ejecta velocities are fairly large, near the escape velocity of the neutron star ($\sim 0.1 - 0.3c$). If the WD is surrounded by a relatively dense circumstellar medium, the ejecta may be slowed down and the light curves powered in part by shock heating (Fryer et al. 2009; Metzger et al. 2009).

While the above white dwarf models may explain a subset of the observational class of RFSNe, in this paper we argue that they cannot explain all such events. We consider in particular the SN 2010X-like transients and highlight two observables that may point to a different origin. The first is the precipitous decline in the post-maximum light curve with no sign, at least within the limits of the observations, of a radioactively powered light curve tail at late times. This suggests that the amount of radioisotopes ejected is quite small. The second is the presence of certain strong spectral features, in particular OI. In this paper, we show that the OI lines in SN 2010X may require a relatively large mass of ejected oxygen, which is difficult to accommodate along with the rapid decline in brightness in a ".Ia" or similar model. A similar estimate of the oxygen mass is discussed by Drout et al. (2013) in an analysis of SN 2005ek.

Some previous studies have considered a core collapse explanation for RFSNe. Moriya et al. (2010) simulate low-energy explosions in massive stars and show that, with proper tuning, only a small amount of mass may be ejected (~ 0.1 M$_\odot$) with most of the star falling back onto a compact remnant (a black hole). The 1D models of Moriya et al. (2010) assume an artificial complete mixing, although the authors speculate that a jet-powered explosion may be able to carry ^{56}Ni to the surface layers. Drout et al. (2013) also discuss the possibility of a low-energy ($0.25 - 0.52$ B) core collapse explanation for SN 2005ek with an inferred ejecta mass of $0.3 - 0.7$ M$_\odot$, a ^{56}Ni mass of 0.03M$_\odot$, citing fallback among a few explanations for such a low-mass ejection. One question this raises is how the radioactive ^{56}Ni, which is usually produced in the dense innermost regions of the star, avoids falling back and instead is ejected with the outer layers of the star.

The common feature of all of the above models has been an unusually low ejected mass and energy. Here, in contrast, we show that the mass and energy of SN 2010X-like events may be typical of Type Ib/c SNe ($M \sim 1-5$ M$_\odot$, $E \sim 1$ B). We attribute the luminosity not to radioactivity but to the thermal energy deposited by the explosion itself. The rapid light curve decline, despite the relatively high ejected mass, can be explained by recombination, which dramatically reduces the effective opacity.

The possibility that some SNe may fail to eject radioactive isotopes has been considered before. Fryer et al. (2009) discuss models of very massive stars ($\gtrsim 20$ M$_\odot$) in which the amount of material that falls back onto the remnant may be quite substantial, i.e. several solar masses. Essentially all of the ^{56}Ni is formed in the innermost layers of the ejecta and falls back, robbing the light curves of energy from radioactive decay and producing very dim events (V and B magnitudes of -13 to -15). Ugliano et al. (2012) indicate that such a large amount of fallback material is unlikely, probably not more than ~ 0.2M$_\odot$, but this may still be enough to accrete most if not all of the radioactive material produced. Dessart et al. (2011) have considered Type Ib models that lack ^{56}Ni and show that they produce relatively short duration, thermally powered light curves with peak luminosities ($\sim 10^{40} - 10^{41}$ ergs s^{-1}).

In this paper, we explore such models of massive star explosions as an explanation for SN 2010X-like events. We first argue that SN 2010X ejected a substantial amount of oxygen, suggestive of the explosion of a stripped-envelope, massive star (§2). We then demonstrate that massive SNe can produce brief, rapidly declining light curves once recombination is taken into account (§3). We then use the radiative transfer code SEDONA (Kasen et al. 2006) to produce synthetic light curves and spectra of simple, 1-D ejecta models, and show that these models can reproduce the SN 2010X light curve, provided that the progenitor star had a large enough radius (§4). In §5, we discuss various progenitor scenarios that may be responsible for this class of SNe.

2 ESTIMATES OF THE EJECTA MASS

Analytical scaling relations are commonly used to estimate the ejecta mass and kinetic energy of observed SNe. For ejecta of mass $M_{\rm ej}$ and velocity v, and assuming a constant opacity κ, the duration of the light curve $t_{\rm sn}$ is set by the effective diffusion time through the expanding ejecta (Arnett 1979):

$$t_{\rm sn} \approx 34 \left(\frac{M_{\rm ej}}{\rm M_\odot}\right)^{1/2} \kappa_{0.1}^{1/2} v_4^{-1/2} \text{ days}, \quad (1)$$

where $v_4 = v/10^4$ km s^{-1} and $\kappa_{0.1} = \kappa/0.1$ cm^2 g^{-1}. We have calibrated the numerical constant based on Type Ia

SNe, which have $v_4 \approx 1, M_{\rm ej} \approx 1.4$ M$_\odot$ and a bolometric light curve width (i.e., rise plus fall) of roughly 40 days (Contardo et al. 2000). The value $\kappa = 0.1$ cm^2 g^{-1} is appropriate for electron scattering in singly ionized helium. It is also similar to the mean opacity due to Doppler broadened lines of iron-group elements, which is the dominant form of opacity in SNe Ia (Pinto & Eastman 2000).

Inverting Equation 1 for the ejecta mass gives

$$M_{\rm ej} \approx 0.0875 \left(\frac{t_{\rm sn}}{10 \text{ days}}\right)^2 v_4 \kappa_{0.1}^{-1} \text{ M}_\odot, \quad (2)$$

which has fostered the belief that RFSNe like SN 2010X represent relatively low mass ejections. Such an argument, however, presumes a constant opacity of $\kappa \sim 0.1$ cm^2 g^{-1}. In fact, the opacity of SN ejecta is highly dependent on the physical state and, as we discuss in the next section, may vary by an order of magnitude depending on the temperature and composition of the ejecta.

It is possible to derive an independent constraint on the ejecta mass using absorption features observed in the spectrum. In particular, SN 2010X showed a strong, broad, and persistent OI triplet feature ($\lambda\lambda\lambda$7772,7774,7775), which would seem to suggest a significant mass of oxygen. In homologously expanding atmospheres, the degree of absorption is quantified by the Sobolev optical depth,

$$\tau_{\rm sob} = \left(\frac{\pi e^2}{m_e c^2}\right) t_{\rm exp} \lambda_0 n_l, \quad (3)$$

where λ_0 is the rest wavelength of the line, $t_{\rm exp}$ the time since explosion, and n_l the number density in the lower level of the atomic transition.

In Figure 1 we plot contours of $\tau_{\rm sob}$ for the OI triplet line as a function of density and temperature for ejecta composed of pure oxygen at $t_{\rm exp} = 30$ days, a time when the oxygen absorption feature is quite prominent in SN 2010X. To estimate n_l we have assumed that the ionization/excitation states were approximately given by local thermodynamic equilibrium (LTE). Figure 1 shows that a density of at least $\rho_{\rm c} \approx 10^{-14}$ g cm^{-3} is required to achieve strong ($\tau_{\rm sob} \gtrsim 1$) absorption in the OI line. This critical density corresponds to the most favorable temperature, $T \approx 5500$ K, at which the level density n_l is highest. For hotter temperatures, oxygen becomes more highly ionized, while for cooler temperatures it is difficult to thermally populate the excited lower level of the OI transition. In these cases, an even higher density is required to make the line optically thick.

We can use this critical OI density to obtain an approximate lower limit on the total ejecta mass of SN 2010X. The February 23 spectrum (close to $t_{\rm exp} \approx 20$ days) showed apparent OI absorption at velocities $\approx 10,000$ km s^{-1}. Assuming that the ejecta density profile is described by a broken power-law (see §4) and that the energy release per unit mass is typical of SNe, $E/M \sim 10^{51}$ ergs/M$_\odot$, the condition $\rho \gtrsim \rho_c$ at $v \approx 10,000$ km s^{-1} implies a total ejecta mass $M_{\rm ej} \gtrsim 0.35$ M$_\odot$. This is likely a significant underestimate, as we have assumed the oxygen layer was composed of 100% oxygen at the ideal temperature of $T \approx 5500$ K. The March 7 spectrum of SN 2010X (near $t_{\rm exp} \approx 30$ days) also shows strong absorption at the same location, which implies $M_{\rm ej} \gtrsim 1.2$ M$_\odot$.

These spectroscopic mass estimates are subject to two important caveats. First, the absorption near 7500 Å may be due in part to MgII (and perhaps FeII) rather than OI lines. Second, the line optical depths may be influenced by non-LTE effects. The lower level of the OI feature is a quasi-stationary state (albeit with a high excitation energy, $\Delta E = 9.14$ eV) such that an LTE description may not be a bad approximation. Nonetheless, it is quite possible that the level population is enhanced by non-thermal excitation by radioactive decay products (Lucy 1991; Dessart et al. 2012), or by time-dependent effects (Dessart & Hillier 2008). As an empirical check of the method, one can examine the constraints for normal SNe Ia. For SN 1994D, for example, the OI feature remained mildly optically thick ($\tau_{\rm sob} \sim 1$) until about 12 days past maximum light ($t_{\rm exp} \approx 30$ days). From this, one calculates a total ejecta mass of $\sim 1-2$ M$_\odot$, which is consistent with the values expected for SNe Ia. The OI feature of SN 2010X at a comparable epoch ($t_{\rm exp} \approx 30$ days) is significantly broader and deeper than that of SN 1994D. We therefore consider it likely that the ejected mass of SN 2010X was comparable to or larger than that of a typical SNe Ia, hence $M_{\rm ej} \gtrsim 1$ M$_\odot$.

The association of SN 2010X with a massive progenitor is strengthened by comparison with core-collapse SNe. Figure 2 shows the SN 2010X spectra with those of SN 1994I, which is considered a fairly typical, if somewhat fast-evolving, Type Ic SNe. The agreement is striking and strongly points to a similar physical origin for the two. Drout et al. (2013) have also noted the spectroscopic resemblance of SN 2005ek to other normal SNe Ic as well as SN 2010X. The light curve of SN 1994I showed a clear radioactive tail, indicating that it ejected ~ 0.07 M$_\odot$ of ^{56}Ni (Young et al. 1995; Iwamoto et al. 1994). We will suggest that SN 2010X was a compositionally similar Type Ib/c SN but did not eject as much ^{56}Ni.

3 OXYGEN PLATEAU SUPERNOVAE

The mass estimates discussed in the last section present a paradox – the narrow light curve of SN 2010X suggests a low $M_{\rm ej}$, while the spectroscopic constraints indicate that $M_{\rm ej}$ may be many times larger. Here we show that the conflicting estimates can be reconciled in a core-collapse model in which the ejecta mass is large ($M \gtrsim 1$ M$_\odot$) but where the effective diffusion time is significantly reduced due to recombination.

The opacity of SN ejecta is highly dependent on the ionization state and so may vary significantly with temperature. In Figure 3, we plot the Rosseland mean opacity (calculated assuming LTE) of SN ejecta of different compositions. We consider in particular a oxygen-neon-magnesium composition (see Table 1) which may be characteristic of the massive, stripped envelope stars believed to be the progenitors of Type Ic SNe. For higher temperatures ($T \gtrsim 6000$ K), the O-Ne-Mg opacity has a characteristic value $\kappa \approx 0.04$ cm^2 g^{-1} When the temperature drops below 6000 K, however, oxygen recombines to neutral, and the opacity drops sharply by more than an order of magnitude. This is because, in the absence of scattering off of free-electrons, photons can escape through the "windows" in wavelength space that occur between the lines, reducing the Rosseland mean opacity. However, the opacity does not drop to zero at $T \lesssim 6000$ K because other elements (such as Mg and Si) with lower ionization potentials remain ionized. For a helium-rich com-

position, recombination occurs at a higher temperature ($\sim 10,000\ K$) due to the higher ionization potential of helium. In contrast, the opacity of ^{56}Ni and its daughter nuclei (^{56}Co and ^{56}Fe), due to the lower ionization potential of the iron group species, maintains a large value as long as $T \gtrsim 3000$ K.

The recombination physics will strongly influence the light curves of SNe composed largely of oxygen. The radiative transfer parallels the well understood effects in Type II plateau SNe (e.g., Grassberg et al. 1971; Dessart & Hillier 2008). Initially, the ejecta are heated and ionized by the passage of the explosion shockwave. As the ejecta expand and cool, however, the material eventually drops below the recombination temperature $T_{\rm i}$ and becomes largely transparent. Because the outer layers of ejecta are the coolest, they recombine first, and a sharp ionization front develops in the ejecta. As time goes on, the ionization front recedes inward in mass coordinates, releasing the stored thermal energy. When this recombination wave reaches the center of the ejecta, the stored energy is exhausted and the light curve should drop off very rapidly, marking the end of the "oxygen-plateau" phase. The analogous case of a helium plateau in Type Ib SN has been discussed by Ensman & Woosley (1988) and Dessart et al. (2011).

Relationships for the timescale and peak luminosity of Type II plateau supernovae, including the effects of recombination, have been determined by Popov (1993) and verified numerically by Kasen & Woosley (2009), who find

$$t_{\rm sn} \approx 120 E_{51}^{-1/6} M_{10}^{1/2} R_{500}^{1/6} \kappa_{0.4}^{1/6} T_{6000}^{-2/3} \text{ days} , \quad (4)$$

$$L_{\rm sn} \approx 1.2 \times 10^{42} E_{51}^{5/6} M_{10}^{-1/2} R_{500}^{2/3} \kappa_{0.4}^{-1/3} T_{6000}^{4/3} \text{ ergs/s} , \quad (5)$$

where $E_{51} = E/10^{51}$ ergs is the explosion energy, $M_{10} = M/(10\ M_\odot)$ is the ejected mass, $R_{500} = R/(500\ R_\odot)$ is the presupernova radius, $\kappa_{0.4} = \kappa/(0.4\ \text{cm}^2\text{g}^{-1})$ is the opacity of the ejecta, and $T_{6000} = T/(6000\ \text{K})$ is the ejecta temperature. The numerical calculations of Kasen & Woosley (2009) actually found a scaling closer to $t_{\rm sn} \propto E^{-1/4}$ rather than $E^{-1/6}$, but otherwise the relations are the same. We can use similar arguments for hydrogen-less supernovae, assuming the luminosity is determined by the recombination temperature of whatever species dominates the ejecta.

Inverting Equations 4 and 5 allows us to solve for the ejecta mass and presupernova radius in terms of observed quantities,

$$M_{\rm ej} \approx 2.9\ L_{42}^{-1} t_{20}^4 v_4^3 \kappa_{0.04}^{-1} T_{6000}^4\ \text{M}_\odot , \quad (6)$$

$$R_0 \approx 12.4\ L_{42}^2 t_{20}^{-2} v_4^{-4} \kappa_{0.04} T_{6000}^{-4}\ \text{R}_\odot . \quad (7)$$

These are very rough estimates, but they demonstrate that, when recombination is accounted for, the light curves of SN 2010X and other RFSNe are consistent with massive ($M_{\rm ej} \gtrsim 1\ \text{M}_\odot$) ejections which powered by shock energy, not radioactivity, provided that the radius of the progenitor star is sufficiently large.

4 RADIATIVE TRANSFER MODELS

To model the light curves and spectra of RFSNe in more detail, we use the time-dependent Monte Carlo code radiative transfer code SEDONA (Kasen et al. 2006). We base our calculations on simple parameterized ejecta models rather than on detailed hydrodynamical simulations, as this allows us to easily control the ejecta mass, kinetic energy, and progenitor star radius. We vary these parameters, in an empirical spirit, in an effort to fit the observations of SN 2010X and constrain its physical properties.

4.1 Ejecta Models

For simplicity, we consider ejecta models that are spherically symmetric and in the homologous expansion phase. Simulations of core-collapse explosions suggest that the ejecta density structure can roughly be described by broken power-law profile (Chevalier 1992),

$$\begin{aligned} \rho_{\rm in}(r,t) &= \zeta_\rho \frac{M}{v_{\rm t}^3 t^3} \frac{r}{v_{\rm t} t}^{-\delta} \text{ for } v < v_t , \\ \rho_{\rm out}(r,t) &= \zeta_\rho \frac{M}{v_{\rm t}^3 t^3} \frac{r}{v_{\rm t} t}^{-n} \text{ for } v \geqslant v_t , \end{aligned} \quad (8)$$

where $v_{\rm t}$ is the velocity at the transition between the two regions,

$$v_{\rm t} = 4.5 \times 10^8 \zeta_v (E_{51}/\text{M}_\odot)^{1/2} \text{cm s}^{-1} . \quad (9)$$

The coefficients ζ_ρ and ζ_v are constants which can be determined by requiring Equation 8 integrate to the specified mass and energy. In our model for SN 2010X, we use $\delta = 1$ and $n = 8$ as they are typical values for core collapse SN and produced reasonable fits to the light curves and spectra.

Immediately following the passage of a core-collapse SN shockwave, the explosion energy is roughly equally split between the kinetic energy and thermal energy of the stellar material. The latter is strongly radiation dominated. Simulations suggest that, before radiative diffusion sets in, the ratio of the radiation energy density to the mass density is nearly constant throughout most of the envelope (Woosley 1988). We therefore take the energy density profile at t_0, the start time of our calculation, to be

$$\epsilon(v,t_0) = \frac{E_0}{2} \frac{\rho(v)}{M} \left(\frac{R_0}{R_{\rm ej}} \right) , \quad (10)$$

where $R_{\rm ej} = v_t t_0$ is the size of the remnant at the start of our transport calculation. This expression assures that the total thermal energy equals $E_0/2$ when $R_{\rm ej} = R_0$; the term in parentheses accounts for losses due to adiabatic expansion prior to the start of our transport calculation. In this model, the initial energy density profile is a broken power law with the same exponents as the mass density. This is reasonably consistent with analytical results that find that the energy density power law in the outer layers is very similar to, though slightly steeper than, the mass density profile (Chevalier 1992).

We assume that the composition of the ejecta is homogenous in two layers. Detailed abundances are given in Table 1. Abundances for the inner layers ($v \leqslant 10000$ km s^{-1}) are typical of an O-Ne-Mg layers of a massive star and taken from the stellar evolution models of Woosley et al. (2002) for a 25 M$_\odot$ pre-supernova star at a mass coordinate of 3.9 M$_\odot$. For the outer layers ($v > 10000$ km s^{-1}) we assume He-rich material with a solar abundances of metals. The inclusion of a helium in the outer layers in fact does not significantly affect the light curves and spectra, as the photosphere at the epochs of interest turns out to be in the O-Ne-Mg layers. For the models in this paper, we assume that no radioactive

isotopes were ejected, so the light curves are solely powered by the energy deposited in the explosion shock wave.

4.2 Synthetic Light Curves and Spectra

We performed radiative transfer calculations for a series of models, in which we vary the three key ejecta parameters: the explosion E, the ejected mass $M_{\rm ej}$, and the presupernova radius R_0. Figure 5 shows how the SDSS r-band light curve changes as we vary each parameter while holding the others fixed. We show the r-band curves for easy comparison to SN 2010X, as this is the band in which we have the most data. The general trends are qualitatively consistent with the scaling relations (Equations 4 and 5). Increasing the explosion energy shortens the light curve duration while increasing the peak luminosity. Raising the mass increases the light curve duration but does not strongly affect its peak luminosity. Finally, a larger presupernova radius increases both the luminosity and duration of the light curve. The light curves resemble those presented in Dessart et al. (2011) for models of Type Ib/c SNe assumed to eject no ^{56}Ni.

In Figure 4 we show a fit to the light curve of SN 2010X, using a model with $M_{\rm ej} = 3.5$ M$_\odot$, $E = 1$ B, and $R_0 = 2 \times 10^{12}$ cm. The model demonstrates that the basic properties of this RFSNe can be explained by the explosion of an ordinary-mass star in which the emission is powered solely by the energy deposited in the explosion shockwave, without any radioactive ^{56}Ni. The assumed radius of the progenitor, however, is significantly larger than that of typical Wolf-Rayet stars, an issue we return to in §5. The short duration of the model light curve reflects the rapid release of radiation energy by the receding recombination wave. The luminosity for the first 25 days (the "oxygen-plateau") is fairly constant, but then drops dramatically as the recombination wave nears the center of the ejecta and the stored radiation energy is exhausted. After day 25, the r-band magnitude drops by more than 3 magnitudes in only 5 days, marking the end of the plateau phase. As no radioisotopes were included, the light curve shows no radioactive tail at late times, and the luminosity continues to drop rapidly.

The light curve fit does not uniquely constrain all three model parameters (M, E, and R_0) as there are essentially only two photometric observables (light curve brightness and duration). We have chosen to show here a model in which the mass and energy are typical of ordinary Type Ic SNe, but other combinations can provide fits of similar quality (see Figure 5). The degeneracy can perhaps be broken by using the observed velocity to constrain the mass energy ratio; however, the photospheric velocity in plateau SNe is set by the location of the recombination front and hence is not necessarily indicative of $v \approx (2E/M)^{1/2}$.

Figure 7 compares the synthetic spectrum (at $t_{\rm exp} = 24$ days) of the same model to the February 23 spectrum of SN 2010X. On the whole, the model does a good job reproducing the major spectral features and in particular predicts significant absorption near the OI triplet. This supports the idea that the composition of the SN 2010X ejecta is consistent with that of a O-Ne-Mg core of a massive star. In detail, however, one notices discrepancies in the position and depth of several features. For instance, the model absorption near 5600 Å, due to the sodium NaID line, is much too weak and has too low a velocity. A similar problem with the NaID line has often been noted in models of Type IIP SNe, and has been explained as resulting from the neglect of time-dependent non-LTE effects (Dessart & Hillier 2008). Thus, while fine-tuning of our ejecta parameters could likely improve the spectral fit, the overall agreement is presumably limited by the simplified nature of the calculations, including the one-dimensional broken power law density structure, the two-zone uniform composition, and the neglect of non-LTE effects.

The identification of the absorption features at 6800 Å and 7000 Å was the subject of some discussion in Kasliwal et al. (2010), who suggest that these features may be due either to lines of AlII or HeI. Our model does not include aluminum, and the helium lines are optically thin, given the lack of non-thermal excitation from radioactivity. Analysis of the Sobolev optical depths suggest that lines of FeII and neutral species (SiI λ7035 and CaI) contribute to the spectral features in this wavelength region. Drout et al. (2013) similarly show that the spectra of SN 2010X-like events can be reasonably fit without invoking aluminum or helium absorption lines.

In Figure 6, we show the spectral time series of SN 2010X alongside select spectra from our model. The general trends are reasonable, but the color evolution is faster in the model. For example, the day 10 model spectrum is bluer than the day 9 observed spectrum, while the day 31 model spectrum is redder than the observed day 36 spectrum. Our radiative transport becomes suspect at later times ($\gtrsim 30$ days) as the ejecta are becoming optically thin and non-LTE effects should become more significant. While the model spectral series does not reproduce every observed spectral feature, we emphasize that we have chosen to limit any fine-tuning of the abundances and explosion parameters in order to fit the data. Further adjustment of the oxygen-rich composition would presumably lead to an improved fit, as has been shown in the modeling of the spectroscopically similar SN 1994I (Sauer et al. 2006).

5 DISCUSSION AND CONCLUSIONS

We have argued that some RFSNe, in particular the SN 2010X-like events, are the result of core-collapse explosion of massive stripped-envelope stars. This contradicts previous suggestions that these events represent low mass, low-energy outbursts from, for example, ".Ia" explosions on white dwarfs. In our picture, the supernova ejected very little radioactive material and the light curve was instead powered by the diffusion of thermal energy deposited by the explosion shock wave. The short duration of the light curve, despite the relatively high ejected mass ($M \sim 3.5$ M$_\odot$), is due to recombination, which dramatically reduces the effective opacity. The evolution is similar to Type IIP supernovae, and the sharp decline of the light curve can be understood as reflecting the end of an "oxygen plateau". Our 1D radiation transport models demonstrate that the observations of SN 2010X are consistent with this scenario. Empirically, the spectral similarity of SN 2010X with the Type Ic SN 1994I strongly suggests that these events have oxygen-dominated ejecta as would be expected in stripped core-collapse SNe.

Other RFSNe may have a similar origin. The light curve of SN 2002bj had a very similar decline rate to that of

SN 2010X, but the peak luminosity was about two magnitudes brighter. The model scalings suggest that the brightness and duration could be reproduced in a Type Ib/c plateau SN with larger progenitor radius and/or higher explosion energy. The spectral features of SN 2002bj were distinct from SN 2010X, perhaps because the ejecta temperatures were higher, but possibly because the composition of the ejecta was different (e.g., helium-rich instead of oxygen-rich). Further modeling is needed to constrain the ejecta properties in detail.

Recently, Drout et al. (2013) presented a detailed analysis of SN 2005ek, which was spectroscopically and photometrically similar to SN 2010X. The late-time R and I band observations of SN 2005ek (at 40 and 70 days after peak) do indicate the presence of a radioactively powered light curve tail. The uncertain bolometric corrections, however, make it difficult to determine the actual gamma-ray trapping rate and hence radioactive mass. The late-time light curve decline is consistent with nearly complete gamma-ray trapping, as might be expected in a massive ($M \sim 3\mathrm{M}_\odot$) event. In this case, the inferred ^{56}Ni mass, while not zero, is very small, $M_{\rm ni} \approx 1 - 4 \times 10^{-3}$ M$_\odot$. The luminosity at the light curve peak would then be attributed to an oxygen-plateau of the sort we have described.

In contrast, Drout et al. (2013) argue that if the ejecta mass and kinetic energy of SN 2005ek were relatively low ($M \approx 0.35 - 0.7$ M$_\odot, E \approx 2.5 - 5.2$ B) then most of the gamma-rays escape at late times and the inferred ^{56}Ni mass is much larger, $M_{\rm ni} \approx 0.03$ M$_\odot$, sufficient to power the light curve peak. It is not clear, however, that such a model can explain the rapid light curve decline after peak. Fink et al. (2013) have calculated radiative transport models for similar scenarios (e.g., model ND3 with $M \approx 0.2$ M$_\odot, E \approx 0.43$ $B, M_{\rm ni} \approx 0.07$ M$_\odot$) and find light curves that decline fairly gradually, dropping by only ~ 1 mag in R-band in the 15 days after peak. This is much more gradual than either SN 2005ek or SN 2010X (which dropped ~ 3 R-band mags in 15 days), suggesting that the radioactively powered model may struggle to explain the rapid decline that characterizes this class of SNe.

The light curve of SN 2002bj poses an even greater challenge for radioactively powered models. This event was significantly brighter than either SN 2005ek and SN 2010X, such that the inferred ^{56}Ni mass would be $M_{\rm ni} \approx 0.15 - 0.25$ M$_\odot$ (Poznanski et al. 2010). To be consistent with the rapid rise and steep decline of the light curve, one would need to assume a small ejecta mass, $M \sim 0.3$ M$_\odot$, such that the ejecta consisted of very little else but ^{56}Ni. This, however, contradicts the observed spectrum, which did not show strong features from iron group elements.

A potentially revealing empirical discriminant of the RFSNe is the ratio of the luminosity measured at peak to that on the radioactive tail. Some events, like SN 2002cx, SN 2005E and SN 2008ha, show a moderate peak-to-tail ratio, similar to SNe Ia and consistent with a light curve powered entirely by radioactivity. In contrast, the events considered here (SN 2005ek, SN 2010X, and SN 2002bj) show a larger peak-to-tail luminosity ratio (or no tail at all) more reminiscent of Type IIP supernova. It is possible that this distinction separates those events powered solely by radioactivity from those with an initial thermally powered oxygen (or helium) plateau.

The RFSNe also are distinguished by their host galaxies. All of SN 2010X, SN 2002bj, and SN 2005ek were found in star-forming galaxies and so are consistent with young stellar populations and massive star progenitors. Other types of RFSNe, however, such as SN 2005E and similar low-luminosity calcium-rich transients have often been found in the remote outskirts of elliptical galaxies, which almost exclusively harbor old stars. For these events, a different model, perhaps based on white dwarf progenitors, may be appropriate.

If correct, the identification of SN 2010X-like events as oxygen plateau SNe has two important implications for core-collapse SNe. The first is that some stripped-envelope SNe may eject a very small amount ($\lesssim 10^{-3}$ M$_\odot$) of radioactive isotopes. This may be because abundant radioactivity was not synthesized in the explosion or because the inner ejecta layers remained bound and fell back unto the compact remnant. The fallback process is not well understood; it has mostly been studied in parameterized 1-D models with an artificial inner boundary condition (e.g., Zhang et al. (2008), but see Ugliano et al. (2012)). Fallback is expected to be most significant in low-energy explosions, but it can also be substantial in more energetic SNe if a strong reverse shock propagates inward and decelerates the inner layers of ejecta (Chevalier 1989; Zhang et al. 2008; Dexter & Kasen 2013). If the progenitor experienced a heavy mass loss episode just prior to explosion (as we discuss below) the interaction of the SN with the CSM could produce a reverse shock which may promote fallback of the inner ejecta.

The second implication of our analysis is that the progenitors of some stripped-envelope SNe may have surprisingly large initial radii, perhaps $R \sim 20$ $R_\odot$ for SN 2010X and perhaps $R \gtrsim 100 R_\odot$ for SN 2002bj. This is considerably larger the expected radii of most Wolf-Rayet (WR) stars, $R_0 \sim$ few R$_\odot$. Recent stellar evolution models suggest that some stars with helium envelopes can have radii on the order of 10 $R_\odot$ (Yoon et al. 2010). However, for SN 2010X we favor a composition dominated by oxygen, not helium. In the absence of some refinement of our understanding of stellar evolution, the large inferred radius presumably requires some mechanism to puff up an oxygen star prior to explosion.

One compelling explanation for the large radius is mass loss shortly before explosion. There are both observational and theoretical indications that instabilities can drive significant outflows from massive stars during the late stages of evolution (Woosley et al. 2007; Smith et al. 2011; Quataert & Shiode 2012; Smith & Arnett 2013). Most studies have focused on mass loss episodes occurring ∼years prior to core collapse, which could explain the most luminous SNe observed (Smith et al. 2007; Gal-Yam 2012; Quimby 2012). If the expelled mass expands at roughly the escape velocity of a compact star (~ 1000 km s^{-1}), it will form a circumstellar shell at rather large radii, $R \sim 10^{15}$ cm. This shell, if it is optically thick, sets the effective "radius" of the progenitor, which can produce a very bright SN light curve ($L \sim 10^{44}$ ergs, see Equation 5).

The much fainter SN 2010X could be explained in a similar way if a circumstellar shell was located at a smaller radius, $R \sim 20$ $R_\odot$. This would imply a much shorter time delay (~ 1 day) between mass loss and explosion. In fact, this dichotomy of timescales could be tied to the basic nu-

clear physics of massive stars; the timescale of the oxygen burning phase is ~ 1 year, while that of the silicon burning phase is ~ 1 day. If mass is lost during silicon burning at ~ 1000 km s^{-1}, the resulting circumstellar material would have reached a radius of $10^{12} - 10^{13}$ cm at the onset of core collapse a day or so later, setting the stage for a SN 2010X-like event. Because the shell is relatively close to the explosion site, and any observational indications of interaction (e.g., narrow emission lines) would only be visible for a short time (~ 1 hour) after explosion.

Quataert & Shiode (2012) and Shiode & Quataert (2013) (see also Smith & Arnett 2013) have presented an explicit mechanism for mass loss related to core fusion. They show that waves excited by vigorous convection during oxygen burning can (under certain circumstances) propagate through the star and deposit of order $10^{47} - 10^{48}$ ergs near the surface, sufficient to unbind ~ 10 M$_\odot$ in a red supergiant. They also show that for stripped-envelope stars, the sound-crossing time is short enough ($\lesssim 1$ day) for this mechanism to operate during silicon burning as well.

To explain the light curve of SN 2010X, the mass in the circumstellar shell (or inflated envelope) must be substantial enough to provide a sufficiently long light curve, which may require $M_{\rm csm} \gtrsim 0.5$ M$_\odot$ (using Equation 4 with a timescale of ~ 20 days, $E \sim 1$ B, and $R \sim 20$ R$_\odot$). The energy needed to drive this amount of material from a compact star is $\gtrsim 5 \times 10^{48}$ ergs. This is $\sim 1\%$ of the total energy released during silicon burning, but most of the fusion energy is lost to neutrinos. In the specific models of Shiode & Quataert (2013), wave driven mass loss in stripped envelope stars only ejects $\lesssim 0.01$ M$_\odot$ of material in the silicon burning phase. However, more efficient mechanisms for tapping the burning energy may be possible (Smith & Arnett 2013). The SN 2010X-like events provide motivation to better understand the very late phases of Type Ib/c SN progenitors.

There may be other ways to expand the effective radius of a stripped-envelope progenitor, perhaps related to stellar mergers or a common envelope phase in a binary system (e.g., Chevalier 2012). Alternatively, a large effective radius could be due to reheating of the SN remnant after it has expanded for a brief time. Dexter & Kasen (2013), for example, explore the possibility that the input of accretion power of a central black hole, fed by fallback material, can produce a diversity of SN light curves.

Though they have previously been seen as weak explosions, our analysis suggests that faint, fast SNe like SN 2010X may have more in common with the most luminous SNe in the Universe, namely the superluminous SNe powered by interaction with circumstellar material. In both cases, the progenitors may be massive stars that have experienced heavy mass loss just prior to explosion. The main distinction in the observed light curve may simply be in the timing of the main pre-SN mass loss episode. Further detailed modeling is needed to investigate the dynamics of the interaction and the variety of outcomes, and to determine whether realistic progenitors can produce core-collapse SNe of this type.

Table 1.

species	inner abundance[a]	outer abundance[b]
H	1.3441e-14	—
He	7.2524e-13	9.8671e-01
Li	—	1.0043e-08
Be	—	1.7418e-10
B	—	4.9905e-09
C	1.3561e-02	2.2179e-03
N	2.3119e-09	7.1266e-04
O	6.5954e-01	5.9003e-03
F	—	3.9087e-07
Ne	1.5747e-01	1.1163e-03
Na	3.4553e-05	3.4553e-05
Mg	2.7580e-02	6.4116e-04
Al	—	5.8630e-05
Si	9.5727e-02	7.3099e-04
P	—	6.7316e-06
S	3.9061e-02	3.7317e-04
Cl	—	4.7954e-06
Ar	4.4617e-03	9.6441e-05
K	—	3.7829e-06
Ca	1.2866e-03	6.5889e-05
Sc	—	3.9365e-08
Ti	2.8182e-06	2.8182e-06
V	—	3.6517e-07
Cr	2.9462e-06	1.6984e-05
Mn	—	1.4106e-05
Fe	1.3033e-03	1.2132e-03
Co	3.4272e-06	3.4272e-06
Ni	7.0975e-05	7.0975e-05

Note. — Mass fractions used for the composition in the radiative transport models. The boundary between inner and outer zones is at 10^9 cm. For some isotopes in the inner layer, the abundance was increased to solar.

[a] Woosley et al. (2002) oxygen/neon-rich composition.

[b] Solar composition from Lodders (2003) with all hydrogen converted to helium.

ACKNOWLEDGMENTS

We would like to thank Maria Drout, Alex Heger, Mansi Kasliwal, Ehud Nakar, Christian Ott, Tony Piro, Dovi Poznanksi, Josh Shiode, Alicia Soderberg, and Eliot Quataert for useful discussion. This work was supported by an NSF Astronomy and Astrophysics Grant (AST-1109896) and by an NSF Division of Astronomical Sciences collaborative research grant AST-1206097. I.K is supported by the Department of Energy National Nuclear Security Administration Stewardship Science Graduate Fellowship. D.K is supported in part by a Department of Energy Office of Nuclear Physics Early Career Award, and by the Director, Office of Energy Research, Office of High Energy and Nuclear Physics, Divisions of Nuclear Physics, of the U.S. Department of Energy under Contract No. DE-AC02-05CH11231. We are grateful for computing time made available the National Energy Research Scientific Computing Center, which is supported by the Office of Science of the U.S. Department of Energy under Contract No. DE-AC02-05CH11231.

REFERENCES

Abdikamalov E. B., Ott C. D., Rezzolla L., Dessart L., Dimmelmeier H., Marek A., Janka H.-T., 2010, Phys. Rev. D, 81, 044012
Arnett W. D., 1979, ApJ, 230, L37
Bildsten L., Shen K. J., Weinberg N. N., Nelemans G., 2007, ApJ, 662, L95
Chevalier R. A., 1989, ApJ, 346, 847
Chevalier R. A., 1992, ApJ, 394, 599
Chevalier R. A., 2012, ApJ, 752, L2
Contardo G., Leibundgut B., Vacca W. D., 2000, A&A, 359, 876
Darbha S., Metzger B. D., Quataert E., Kasen D., Nugent P., Thomas R., 2010, MNRAS, 409, 846
Dessart L., Burrows A., Ott C. D., Livne E., Yoon S.-C., Langer N., 2006, ApJ, 644, 1063
Dessart L., Hillier D. J., 2008, MNRAS, 383, 57
Dessart L., Hillier D. J., Li C., Woosley S., 2012, MNRAS, 424, 2139
Dessart L., Hillier D. J., Livne E., Yoon S.-C., Woosley S., Waldman R., Langer N., 2011, MNRAS, 414, 2985
Dexter J., Kasen D., 2013, ApJ, 772, 30
Drout M. R., Soderberg A. M., Mazzali P. A., Parrent J. T., Margutti R., Milisavljevic D., Sanders N. E., Chornock R., Foley R. J., Kirshner R. P., Filippenko A. V., Li W., Brown P. J., Cenko S. B., Chakraborti S., Challis P., 2013, ApJ, 774, 58
Ensman L. M., Woosley S. E., 1988, ApJ, 333, 754
Fink M., Kromer M., Seitenzahl I. R., Ciaraldi-Schoolmann F., Roepke F. K., Sim S. A., Pakmor R., Ruiter A. J., Hillebrandt W., 2013, ArXiv e-prints
Foley R. J., Challis P. J., Chornock R., Ganeshalingam M., Li W., Marion G. H., Morrell N. I., Pignata G., Stritzinger M. D., Silverman J. M., Wang X., Anderson J. P., Filippenko A. V., Freedman W. L., Hamuy M., Jha S. W., Kirshner R. P., 2013, ApJ, 767, 57
Fryer C. L., Brown P. J., Bufano F., Dahl J. A., Fontes C. J., Frey L. H., Holland S. T., Hungerford A. L., Immler S., Mazzali P., Milne P. A., Scannapieco E., Weinberg N., Young P. A., 2009, ApJ, 707, 193
Gal-Yam A., 2012, Science, 337, 927
Grassberg E. K., Imshennik V. S., Nadyozhin D. K., 1971, Ap&SS, 10, 28
Iwamoto K., Nomoto K., Hoflich P., Yamaoka H., Kumagai S., Shigeyama T., 1994, ApJ, 437, L115
Kasen D., Thomas R. C., Nugent P., 2006, ApJ, 651, 366
Kasen D., Woosley S. E., 2009, ApJ, 703, 2205
Kasliwal M. M., Kulkarni S. R., Gal-Yam A., Nugent P. E., Sullivan M., Bildsten L., Yaron O., Perets H. B., Arcavi I., Ben-Ami S., Bhalerao V. B., Bloom J. S., Cenko S. B., Filippenko A. V., Frail D. A., Ganeshalingam M., Horesh A., Howell D. A., 2012, ApJ, 755, 161
Kasliwal M. M., Kulkarni S. R., Gal-Yam A., Yaron O., Quimby R. M., Ofek E. O., Nugent P., Poznanski D., Jacobsen J., Sternberg A., Arcavi I., Howell D. A., Sullivan M., Rich D. J., Burke P. F., Brimacombe J., Milisavljevic D., Fesen R., 2010, ApJ, 723, L98
Kawabata K. S., Maeda K., Nomoto K., Taubenberger S., Tanaka M., Deng J., Pian E., Hattori T., Itagaki K., 2010, Nature, 465, 326
Kromer M., Fink M., Stanishev V., Taubenberger S., Ciaraldi-Schoolman F., Pakmor R., Röpke F. K., Ruiter A. J., Seitenzahl I. R., Sim S. A., Blanc G., Elias-Rosa N., Hillebrandt W., 2013, MNRAS, 429, 2287
Lodders K., 2003, ApJ, 591, 1220
Lucy L. B., 1991, ApJ, 383, 308
Metzger B. D., Piro A. L., Quataert E., 2009, MNRAS, 396, 1659
Moriya T., Tominaga N., Tanaka M., Nomoto K., Sauer D. N., Mazzali P. A., Maeda K., Suzuki T., 2010, ApJ, 719, 1445
Perets H. B., Gal-Yam A., Mazzali P. A., Arnett D., Kagan D., Filippenko A. V., Li W., Arcavi I., Cenko S. B., Fox D. B., Leonard D. C., Moon D.-S., Sand D. J., Soderberg A. M., Anderson J. P., James P. A., Foley R. J., Ganeshalingam M., Ofek E. O., 2010, Nature, 465, 322
Pinto P. A., Eastman R. G., 2000, ApJ, 530, 757
Popov D. V., 1993, ApJ, 414, 712
Poznanski D., Chornock R., Nugent P. E., Bloom J. S., Filippenko A. V., Ganeshalingam M., Leonard D. C., Li W., Thomas R. C., 2010, Science, 327, 58
Quataert E., Shiode J., 2012, MNRAS, 423, L92
Quimby R. M., 2012, in Death of Massive Stars: Supernovae and Gamma-Ray Bursts Vol. 279 of IAU Symposium, Superluminous Supernovae. pp 22–28
Sauer D. N., Mazzali P. A., Deng J., Valenti S., Nomoto K., Filippenko A. V., 2006, MNRAS, 369, 1939
Shen K. J., Kasen D., Weinberg N. N., Bildsten L., Scannapieco E., 2010, ApJ, 715, 767
Shiode J. H., Quataert E., 2013, ArXiv e-prints
Smith N., Arnett D., 2013, ArXiv e-prints
Smith N., Li W., Filippenko A. V., Chornock R., 2011, MNRAS, 412, 1522
Smith N., Li W., Foley R. J., Wheeler J. C., Pooley D., Chornock R., Filippenko A. V., Silverman J. M., Quimby R., Bloom J. S., Hansen C., 2007, ApJ, 666, 1116
Ugliano M., Janka H.-T., Marek A., Arcones A., 2012, ApJ, 757, 69
Woosley S. E., 1988, ApJ, 330, 218
Woosley S. E., Blinnikov S., Heger A., 2007, Nature, 450, 390
Woosley S. E., Heger A., Weaver T. A., 2002, Reviews of

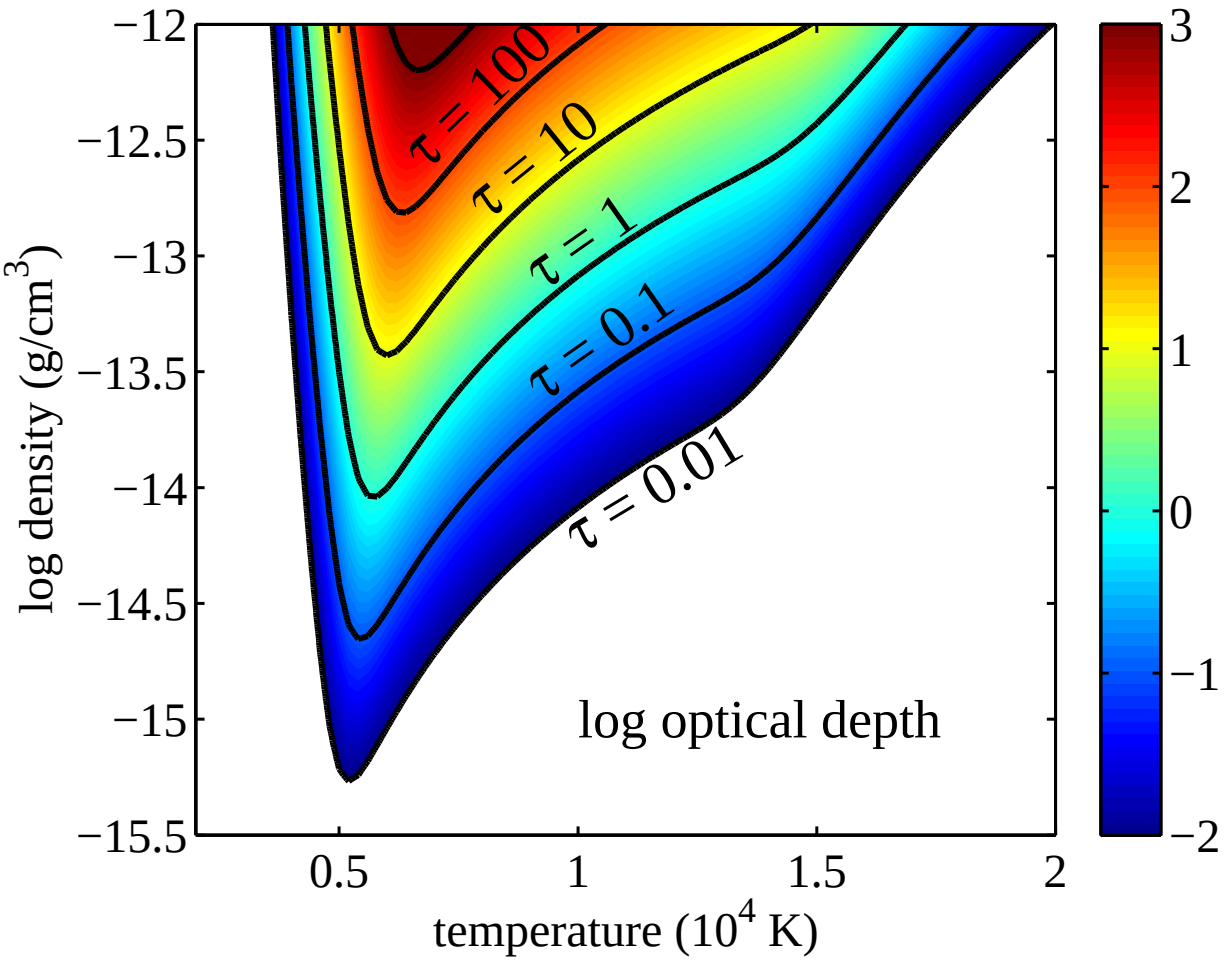

Figure 1. Logarithmic Sobolev optical depth of the combined OI λλλ7772,7774,7775 triplet line as a function of density and temperature for a 100% oxygen composition at $t_{\rm exp}$= 30 days. Black lines indicate curves of constant optical depth. The lowest point in the $\tau = 1$ curve occurs at $\rho_c \approx 10^{-14}$ g/cm^3, which is taken to give the lowest possible density needed to see the OI absorption.

Modern Physics, 74, 1015
Yoon S.-C., Woosley S. E., Langer N., 2010, ApJ, 725, 940
Young T. R., Baron E., Branch D., 1995, ApJ, 449, L51
Zhang W., Woosley S. E., Heger A., 2008, ApJ, 679, 639

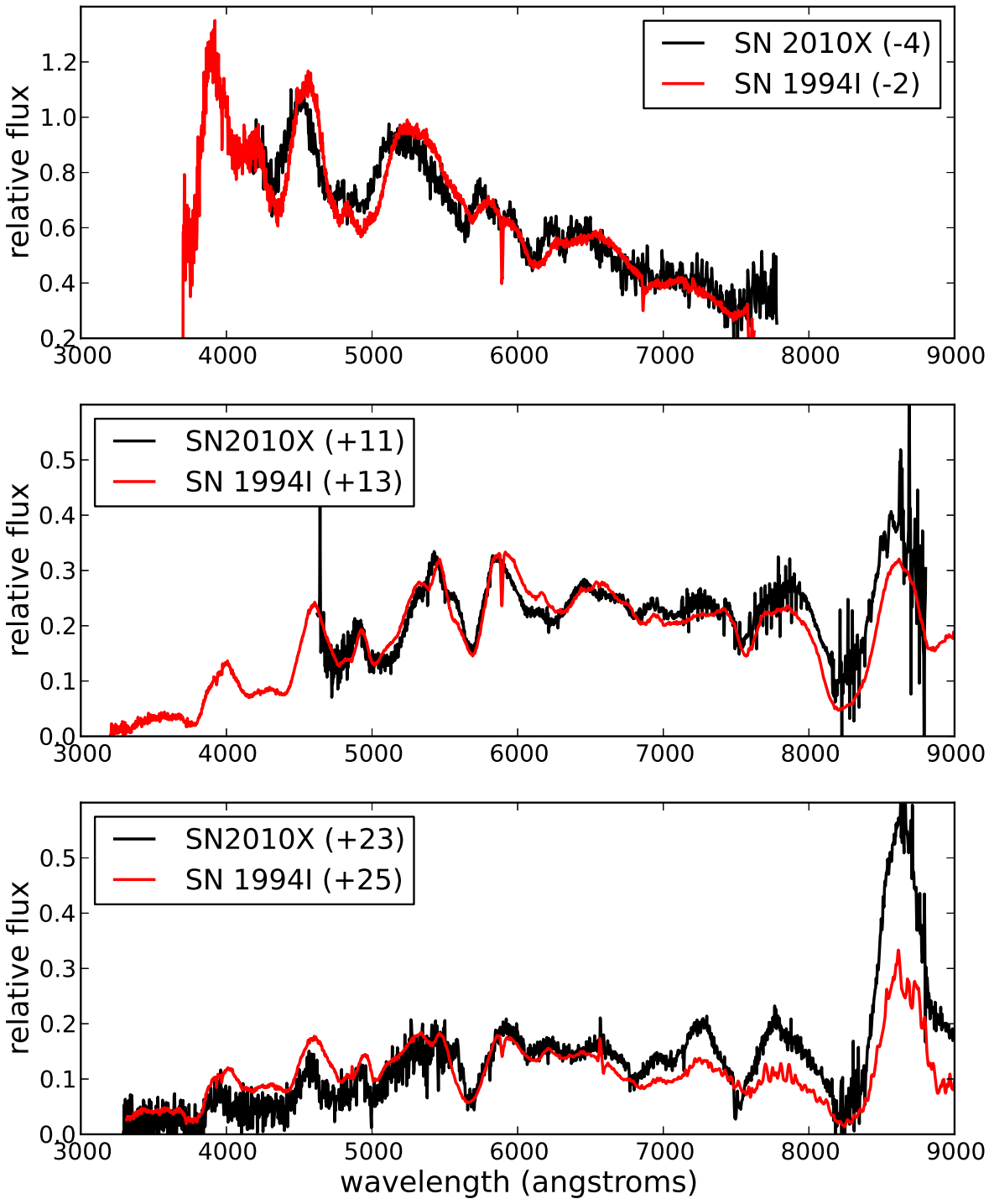

Figure 2. Comparison of the multi-epoch spectra of the Type Ic SN 1994I to those of SN 2010X. Times since B-band maximum are listed. The strong spectral similarity may indicate a similar physical origin.

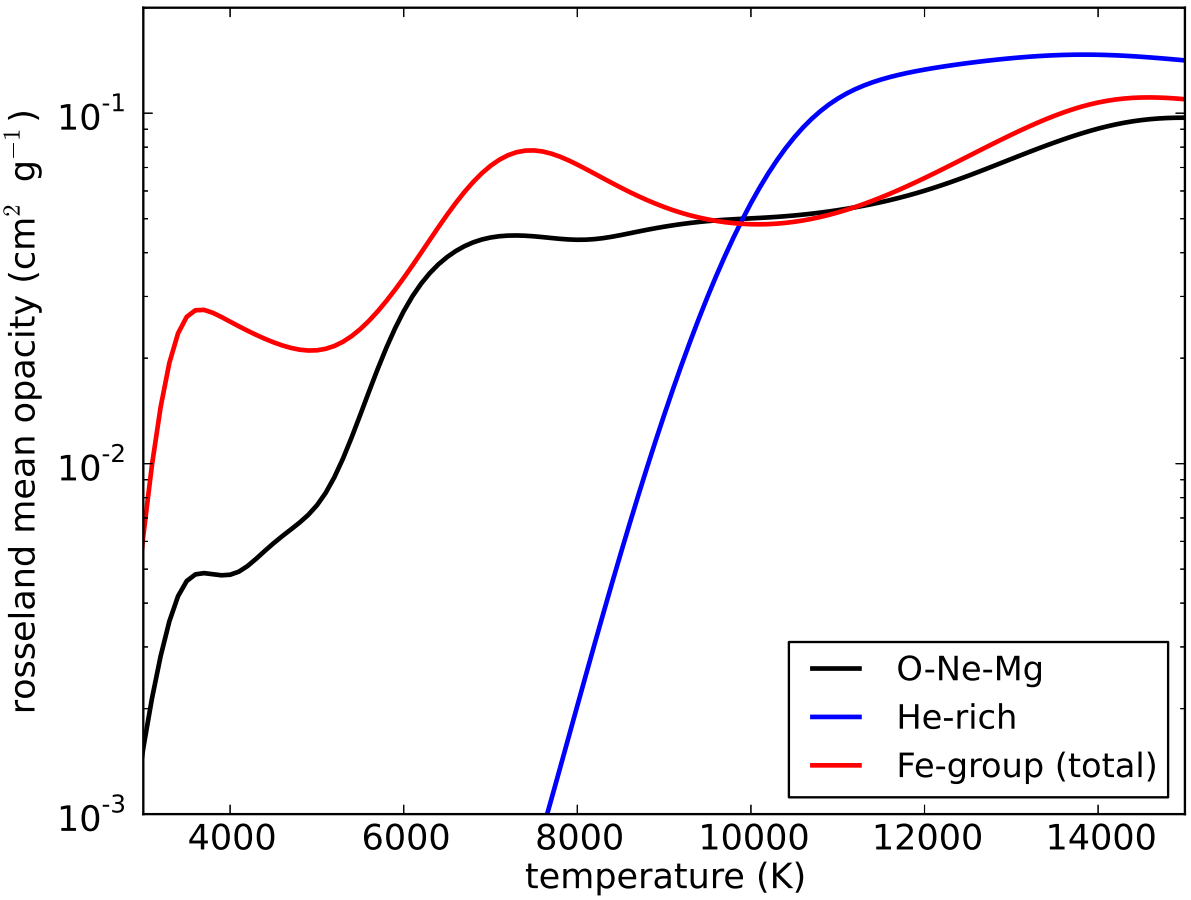

Figure 3. Calculated Rosseland mean opacity (for SN ejecta of different compositions) as a function of temperature for supernova ejecta at a density $\rho = 10^{-13}$ g cm^{-3} and $t_{\rm exp} = 10$ days. The main opacities included are electron scattering and line expansion opacity.

.

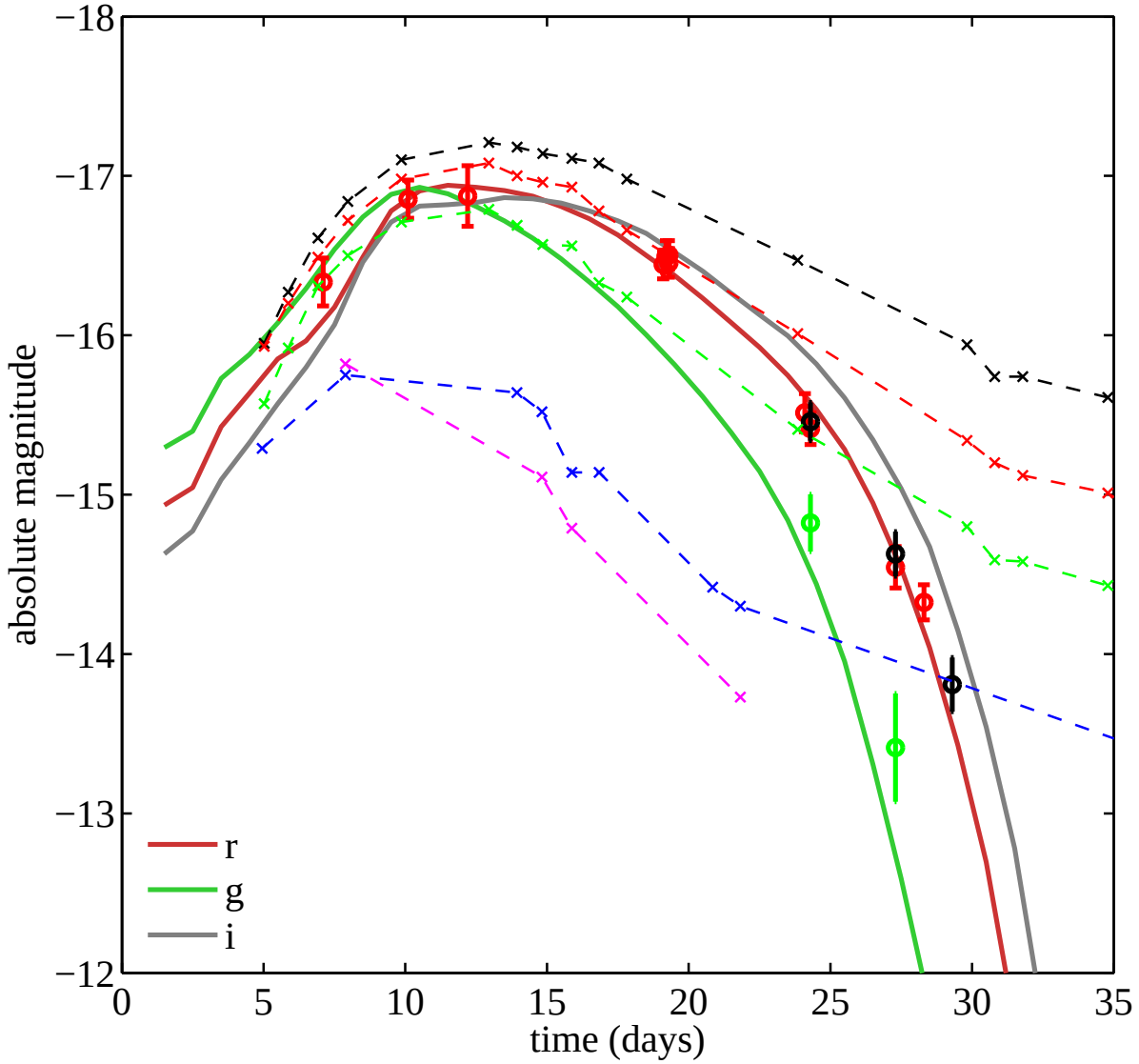

Figure 4. Light curves in g, r, and i calculated for a pure explosion model of SN 2010X, plotted against the data. This model was obtained with $M_{\rm ej} = 3.5$ M$_\odot$, $E_{51} = 1$ B, and $R_0 = 2 \times 10^{12}$ cm. Dotted lines show light curves in $BVRI$ for SN 1994I, a typical SN Ic, for comparison.

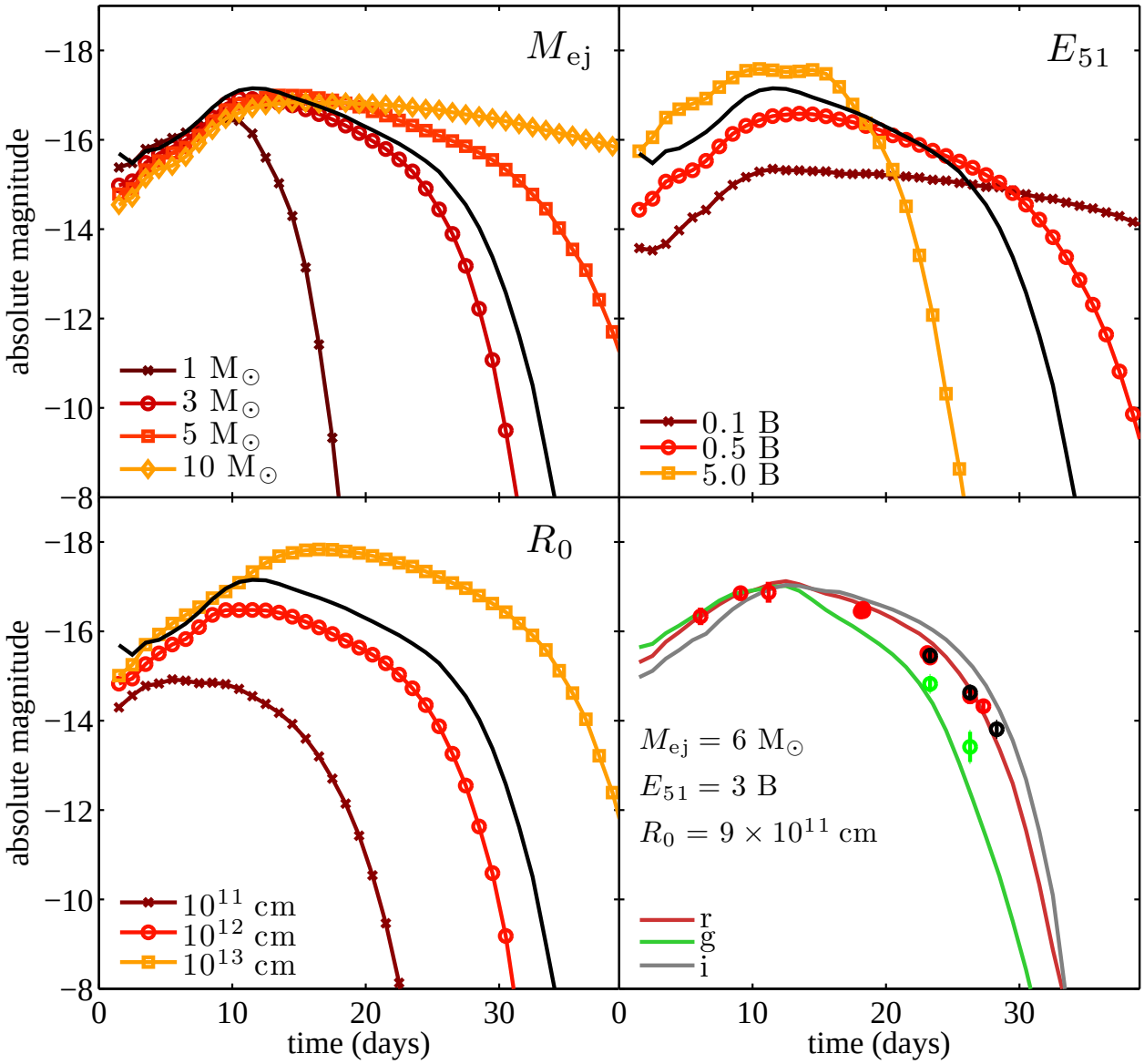

Figure 5. Calculated light curves using parameter variations around our fiducial ejecta model for SN 2010X, which has parameters $M_{\rm ej} = 3.5$ M$_\odot$, $E_{51} = 1$ B, and $R_0 = 2 \times 10^{12}$ cm. Top left: light curve calculations holding all parameters constant except ejecta mass. Top right: same as the top left panel but with varying explosion energy. Bottom left: same as top right and top left panels but with varying presupernova radius. Bottom right: an alternative model that fits the data fairly well with parameters $M_{\rm ej} = 6$ M$_\odot$, $E_{51} = 3$ B, and $R_0 = 9 \times 10^{11}$ cm. This demonstrates the degeneracy in our approach and that the light curves could be fit with a range of parameters.

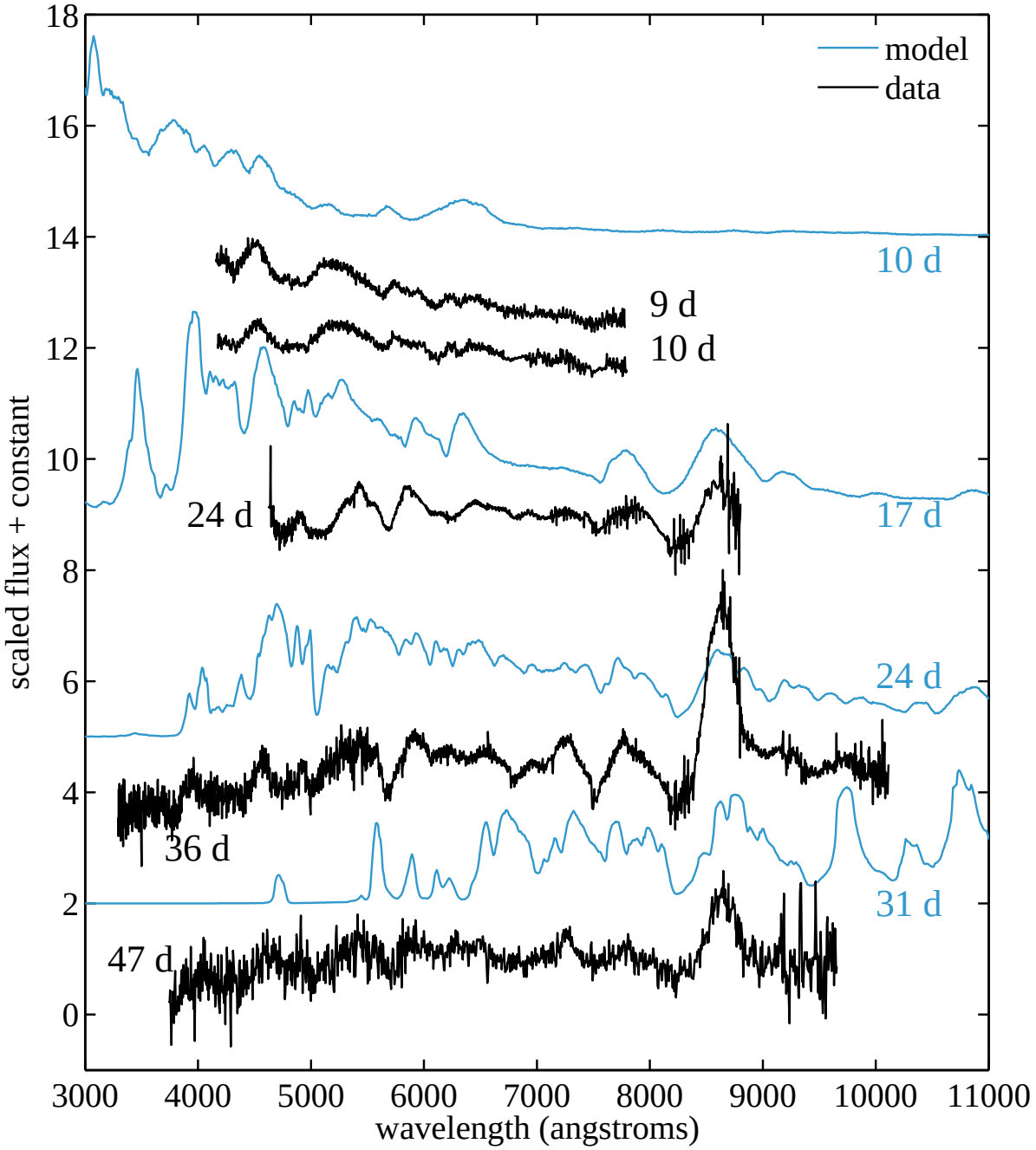

Figure 6. Time series of selected synthetic spectra of our fiducial ejecta model of Figure 4 compared the observed data of SN 2010X showing the evolution of the oxygen line and other prominent features.

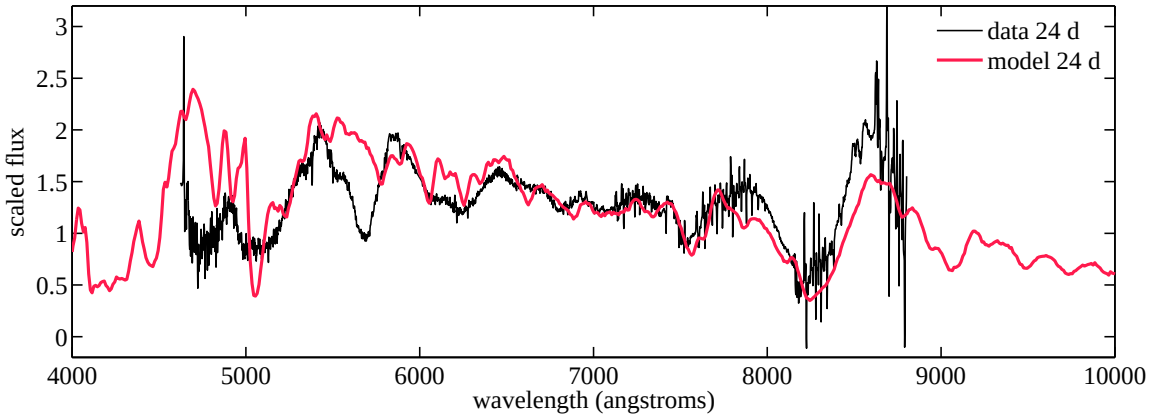

Figure 7. Selected spectrum calculated from our fiducial ejecta model of Figure 4 shown against observed data. The overall shape is similar, and most of the important spectral features are reproduced. Discrepancies may arise from our assumption of LTE, simplified power-law density structure, or the untuned abundances assumed.